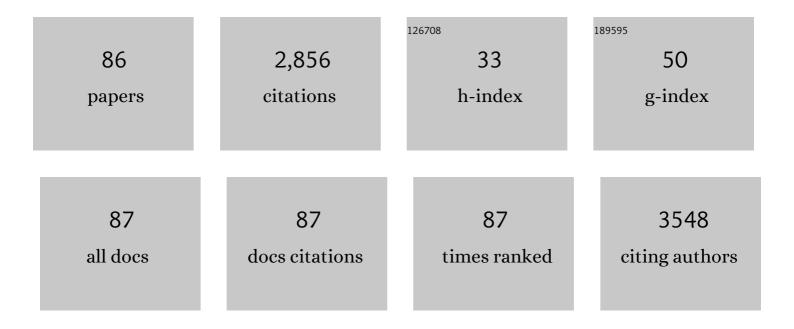
## List of Publications by Year in descending order

Source: https://exaly.com/author-pdf/3117918/publications.pdf Version: 2024-02-01



LUNUE LI

#	Article	IF	CITATIONS
1	Simultaneous Control of Light Polarization and Phase Distributions Using Plasmonic Metasurfaces. Advanced Functional Materials, 2015, 25, 704-710.	7.8	178
2	Planar chiral metasurfaces with maximal and tunable chiroptical response driven by bound states in the continuum. Nature Communications, 2022, 13, .	5.8	131
3	Highâ€Qualityâ€Factor Midâ€Infrared Toroidal Excitation in Folded 3D Metamaterials. Advanced Materials, 2017, 29, 1606298.	11.1	117
4	Demonstration of Orbital Angular Momentum Multiplexing and Demultiplexing Based on a Metasurface in the Terahertz Band. ACS Photonics, 2018, 5, 1726-1732.	3.2	111
5	Directly patterned substrate-free plasmonic "nanograter―structures with unusual Fano resonances. Light: Science and Applications, 2015, 4, e308-e308.	7.7	105
6	Spin-Selective Transmission in Chiral Folded Metasurfaces. Nano Letters, 2019, 19, 3432-3439.	4.5	89
7	Subâ€5 nm Metal Nanogaps: Physical Properties, Fabrication Methods, and Device Applications. Small, 2019, 15, e1804177.	5.2	81
8	Highâ€Performance Broadband Circularly Polarized Beam Deflector by Mirror Effect of Multinanorod Metasurfaces. Advanced Functional Materials, 2015, 25, 5428-5434.	7.8	69
9	Enhanced polarization-sensitive terahertz emission from vertically grown graphene by a dynamical photon drag effect. Nanoscale, 2017, 9, 10301-10311.	2.8	62
10	Temperature-dependent Raman investigation on suspended graphene: Contribution from thermal expansion coefficient mismatch between graphene and substrate. Carbon, 2016, 104, 27-32.	5.4	61
11	Electromechanically reconfigurable optical nano-kirigami. Nature Communications, 2021, 12, 1299.	5.8	61
12	Quasi-2D Transport and Weak Antilocalization Effect in Few-layered VSe <sub>2</sub> . Nano Letters, 2019, 19, 4551-4559.	4.5	60
13	Three Dimensional Hybrids of Vertical Graphene-nanosheet Sandwiched by Ag-nanoparticles for Enhanced Surface Selectively Catalytic Reactions. Scientific Reports, 2015, 5, 16019.	1.6	59
14	Single Grain Boundary Break Junction for Suspended Nanogap Electrodes with Gapwidth Down to 1–2 nm by Focused Ion Beam Milling. Advanced Materials, 2015, 27, 3002-3006.	11.1	59
15	Fano resonance Rabi splitting of surface plasmons. Scientific Reports, 2017, 7, 8010.	1.6	57
16	Realization of a near-infrared active Fano-resonant asymmetric metasurface by precisely controlling the phase transition of Ge <sub>2</sub> Sb <sub>2</sub> Te <sub>5</sub> . Nanoscale, 2020, 12, 8758-8767.	2.8	57
17	Thickness-Dependently Enhanced Photodetection Performance of Vertically Grown SnS <sub>2</sub> Nanoflakes with Large Size and High Production. ACS Applied Materials & Interfaces, 2018, 10, 18073-18081.	4.0	56
18	Robust adhesion of flower-like few-layer graphene nanoclusters. Scientific Reports, 2012, 2, 511.	1.6	55

#	Article	IF	CITATIONS
19	Broadband diodelike asymmetric transmission of linearly polarized light in ultrathin hybrid metamaterial. Applied Physics Letters, 2014, 105, .	1.5	54
20	Bidirectional Perfect Absorber Using Free Substrate Plasmonic Metasurfaces. Advanced Optical Materials, 2017, 5, 1700152.	3.6	52
21	Single-Layer Plasmonic Metasurface Half-Wave Plates with Wavelength-Independent Polarization Conversion Angle. ACS Photonics, 2017, 4, 2061-2069.	3.2	48
22	Graphene–metamaterial hybridization for enhanced terahertz response. Carbon, 2014, 78, 102-112.	5.4	47
23	Thick solid electrolyte interphases grown on silicon nanocone anodes during slow cycling and their negative effects on the performance of Li-ion batteries. Nanoscale, 2015, 7, 7651-7658.	2.8	43
24	3D conductive coupling for efficient generation of prominent Fano resonances in metamaterials. Scientific Reports, 2016, 6, 27817.	1.6	43
25	Anisotropic expansion and size-dependent fracture of silicon nanotubes during lithiation. Journal of Materials Chemistry A, 2019, 7, 15113-15122.	5.2	41
26	Ultrafast carrier transfer evidencing graphene electromagnetically enhanced ultrasensitive SERS in graphene/Ag-nanoparticles hybrid. Carbon, 2017, 122, 98-105.	5.4	40
27	Excitation of ultrasharp trapped-mode resonances in mirror-symmetric metamaterials. Physical Review B, 2016, 93, .	1.1	39
28	Folding 2D Structures into 3D Configurations at the Micro/Nanoscale: Principles, Techniques, and Applications. Advanced Materials, 2019, 31, e1802211.	11.1	39
29	Simultaneous excitation of extremely high-Q-factor trapped and octupolar modes in terahertz metamaterials. Optics Express, 2017, 25, 15938.	1.7	38
30	Nanocracking and metallization doubly defined large-scale 3D plasmonic sub-10 nm-gap arrays as extremely sensitive SERS substrates. Nanoscale, 2018, 10, 3171-3180.	2.8	38
31	Intrinsic Chirality and Multispectral Spinâ€5elective Transmission in Folded Etaâ€5haped Metamaterials. Advanced Optical Materials, 2020, 8, 1901448.	3.6	36
32	Surface Plasmon Polariton Mediated Multiple Toroidal Resonances in 3D Folding Metamaterials. ACS Photonics, 2017, 4, 2650-2658.	3.2	35
33	Wafer‣cale Double‣ayer Stacked Au/Al <sub>2</sub> O <sub>3</sub> @Au Nanosphere Structure with Tunable Nanospacing for Surfaceâ€Enhanced Raman Scattering. Small, 2014, 10, 3933-3942.	5.2	33
34	Multidimensional Image and Beam Splitter Based on Hyperbolic Metamaterials. Nano Letters, 2021, 21, 1792-1799.	4.5	32
35	Giant Intrinsic Chirality in Curled Metasurfaces. ACS Photonics, 2020, 7, 3415-3422.	3.2	30
36	A Well-Defined Silicon Nanocone–Carbon Structure for Demonstrating Exclusive Influences of Carbon Coating on Silicon Anode of Lithium-Ion Batteries. ACS Applied Materials & Interfaces, 2017, 9, 2806-2814.	4.0	29

#	Article	IF	CITATIONS
37	Dynamic Display of Full-Stokes Vectorial Holography Based on Metasurfaces. ACS Photonics, 2021, 8, 1746-1753.	3.2	29
38	Tunable near-infrared perfect absorber based on the hybridization of phase-change material and nanocross-shaped resonators. Applied Physics Letters, 2018, 113, .	1.5	27
39	Subwavelength optical localization with toroidal excitations in plasmonic and <scp>Mie</scp> metamaterials. InformaÄnÃ-Materiály, 2021, 3, 577-597.	8.5	27
40	Polarizationâ€Multiplexed Silicon Metasurfaces for Multiâ€Channel Visible Light Modulation. Advanced Functional Materials, 2022, 32, .	7.8	26
41	Multiplexed Generation of Generalized Vortex Beams with Onâ€Demand Intensity Profiles Based on Metasurfaces. Laser and Photonics Reviews, 2022, 16, .	4.4	25
42	Broadband and Polarization-Insensitive Absorption Based on a Set of Multisized Fabry–Perot-like Resonators. Journal of Physical Chemistry C, 2019, 123, 13856-13862.	1.5	24
43	Titanium dioxide metasurface manipulating high-efficiency and broadband photonic spin Hall effect in visible regime. Nanophotonics, 2020, 9, 4327-4335.	2.9	24
44	Vertical few-layer graphene/metalized Si-nanocone arrays as 3D electrodes for solid-state supercapacitors with large areal capacitance and superior rate capability. Applied Surface Science, 2017, 404, 238-245.	3.1	23
45	Correlated triple hybrid amplitude and phase holographic encryption based on a metasurface. Photonics Research, 2022, 10, 678.	3.4	23
46	Full-Stokes polarization transformations and time sequence metasurface holographic display. Photonics Research, 2022, 10, 1031.	3.4	23
47	Effect of inhomogeneity and plasmons on terahertz radiation from GaAs (100) surface coated with rough Au film. Applied Surface Science, 2013, 285, 853-857.	3.1	21
48	Diameter-optimized high-order waveguide nanorods for fluorescence enhancement applied in ultrasensitive bioassays. Nanoscale, 2019, 11, 14322-14329.	2.8	21
49	Generation of Airy beam arrays in real and K spaces based on a dielectric metasurface. Optics Express, 2021, 29, 18781.	1.7	21
50	Floral-clustered few-layer graphene nanosheet array as high performance field emitter. Nanoscale, 2012, 4, 6383.	2.8	20
51	Broadband cross-polarization conversion by symmetry-breaking ultrathin metasurfaces. Applied Physics Letters, 2017, 111, 241108.	1.5	20
52	Asymmetrical Chirality in 3D Bended Metasurface. Advanced Functional Materials, 2021, 31, 2100689.	7.8	20
53	Circular-Photon-Drag-Effect-Induced Elliptically Polarized Terahertz Emission from Vertically Grown Graphene. Physical Review Applied, 2019, 12, .	1.5	19
54	Multispectral plasmon-induced transparency in hyperfine terahertz meta-molecules. Journal of Physics Condensed Matter, 2016, 28, 445002.	0.7	17

#	Article	IF	CITATIONS
55	Controllable Polarization and Diffraction Modulated Multiâ€Functionality Based on Metasurface. Advanced Optical Materials, 2022, 10, .	3.6	17
56	Multiplexed Nondiffracting Nonlinear Metasurfaces. Advanced Functional Materials, 2020, 30, 1910744.	7.8	16
57	Independent Light Field Manipulation in Diffraction Orders of Metasurface Holography. Laser and Photonics Reviews, 2022, 16, .	4.4	16
58	Side-by-side observation of the interfacial improvement of vertical graphene-coated silicon nanocone anodes for lithium-ion batteries by patterning technology. Nanoscale, 2017, 9, 17241-17247.	2.8	14
59	Ultrafast terahertz response in photoexcited, vertically grown few-layer graphene. Applied Physics Letters, 2016, 108, .	1.5	13
60	Direct Experimental Evidence of Biomimetic Surfaces with Chemical Modifications Interfering with Adhesive Protein Adsorption. Molecules, 2019, 24, 27.	1.7	13
61	Independent tuning of bright and dark meta-atoms with phase change materials on EIT metasurfaces. Nanoscale, 2020, 12, 10065-10071.	2.8	13
62	Rapid templated fabrication of large-scale, high-density metallic nanocone arrays and SERS applications. Journal of Materials Chemistry C, 2014, 2, 9987-9992.	2.7	12
63	Rapid Bending Origami in Micro/Nanoscale toward a Versatile 3D Metasurface. Laser and Photonics Reviews, 2020, 14, 1900179.	4.4	12
64	Precise tailoring of multiple nanostructures based on atomic layer assembly via versatile soft-templates. Nano Today, 2021, 38, 101145.	6.2	12
65	Large-scale ordered silicon microtube arrays fabricated by Poisson spot lithography. Nanotechnology, 2011, 22, 395301.	1.3	11
66	Single-crystal SnO2nanoshuttles: shape-controlled synthesis, perfect flexibility and high-performance field emission. Nanotechnology, 2011, 22, 505601.	1.3	11
67	Arbitrary amplitude and phase control in visible by dielectric metasurface. Optics Express, 2022, 30, 13530.	1.7	11
68	The design and performance of hydrogen-terminated diamond metal-oxide-semiconductor field-effect transistors with high k oxide HfO2. Micro and Nano Engineering, 2020, 6, 100046.	1.4	10
69	Rapidly fabricating large-scale plasmonic silver nanosphere arrays with sub-20Ânm gap on Si-pyramids by inverted annealing for highly sensitive SERS detection. RSC Advances, 2017, 7, 11578-11584.	1.7	9
70	Single-shot phase retrieval based on anisotropic metasurface. Applied Physics Letters, 2022, 120, .	1.5	8
71	Dual-gate field effect transistor based on ZnO nanowire with high-K gate dielectrics. Microelectronic Engineering, 2012, 98, 343-346.	1.1	7
72	Thickness dependence of superconductivity in single-crystal Ta4Pd3Te16 nanoribbons. Applied Physics Letters, 2018, 113, .	1.5	7

#	Article	IF	CITATIONS
73	Plasmonic Hybrids of MoS2 and 10-nm Nanogap Arrays for Photoluminescence Enhancement. Micromachines, 2020, 11, 1109.	1.4	7
74	Flexible Confinement and Manipulation of Mie Resonances via Nano Rectangular Hollow Metasurfaces. Advanced Optical Materials, 2022, 10, .	3.6	7
75	Two Kinds of Metastable Structures in an Epitaxial Lanthanum Cobalt Oxide Thin Film. Inorganic Chemistry, 2019, 58, 13440-13445.	1.9	6
76	Transfer-free synthesis of multilayer graphene on silicon nitride using reusable gallium catalyst. Diamond and Related Materials, 2019, 91, 112-118.	1.8	5
77	Abnormal Rheological Phenomena in Newtonian Fluids in Electroosmotic Flows in a Nanocapillary. Langmuir, 2018, 34, 15203-15210.	1.6	4
78	Micro-Defects in Monolayer MoS2 Studied by Low-Temperature Magneto-Raman Mapping. Journal of Physical Chemistry C, 2020, 124, 17418-17422.	1.5	4
79	Plasmonic Effect on the Magneto-Optical Property of Monolayer WS2 Studied by Polarized-Raman Spectroscopy. Applied Sciences (Switzerland), 2021, 11, 1599.	1.3	3
80	Bidirectional Origami Inspiring Versatile 3D Metasurface. Advanced Materials Technologies, 2022, 7, .	3.0	3
81	Atomic Layer Assembly Based on Sacrificial Templates for 3D Nanofabrication. Micromachines, 2022, 13, 856.	1.4	3
82	Bond length fluctuation in perovskite chromate SrCrO3. Journal of Applied Physics, 2020, 127, 075106.	1.1	2
83	Strain lithography for two-dimensional materials by electron irradiation. Applied Physics Letters, 2022, 120, .	1.5	2
84	Interdigitated silver nanoelectrode arrays: a surface-enhanced Raman scattering platform for monitoring the reorientation of molecules under an external electric field. Journal of Micromechanics and Microengineering, 2019, 29, 124002.	1.5	1
85	High sensitive refractive index sensor based on spatial symmetry breaking Fano metamaterials fabricated by ion beam irradiation. Micro and Nano Engineering, 2020, 9, 100076.	1.4	1
86	Semi-custom methodology to fabricate transmission electron microscopy chip for in situ characterization of nanodevices and nanomaterials. Science China Technological Sciences, 0, , 1.	2.0	0